JACC: BASIC TO TRANSLATIONAL SCIENCE VOL. ■, NO. ■, 2023

ORIGINAL RESEARCH

Left Atrial Glucose Metabolism Evaluation by ^{18}F-FDG-PET in Persistent Atrial Fibrillation and in Sinus Rhythm

Sébastien Marchandise, MD,[a,b] Véronique Roelants, MD, PhD,[c,d] Tristan Raoult, MD,[a,b] Quentin Garnir, MD,[a] Christophe Scavée, MD,[a,b] Varnavas Varnavas, MD PhD,[a,b] Aurélien Wauters, MD, PhD,[a,b] Damien Gruson, MD, PhD,[a,b] Eric Nellessen, MD,[a,b] Michel Hesse, PhD,[c,d] Christophe Beauloye, MD, PhD,[a,b] Bernhard L. Gerber, MD, PhD[a,b]

VISUAL ABSTRACT

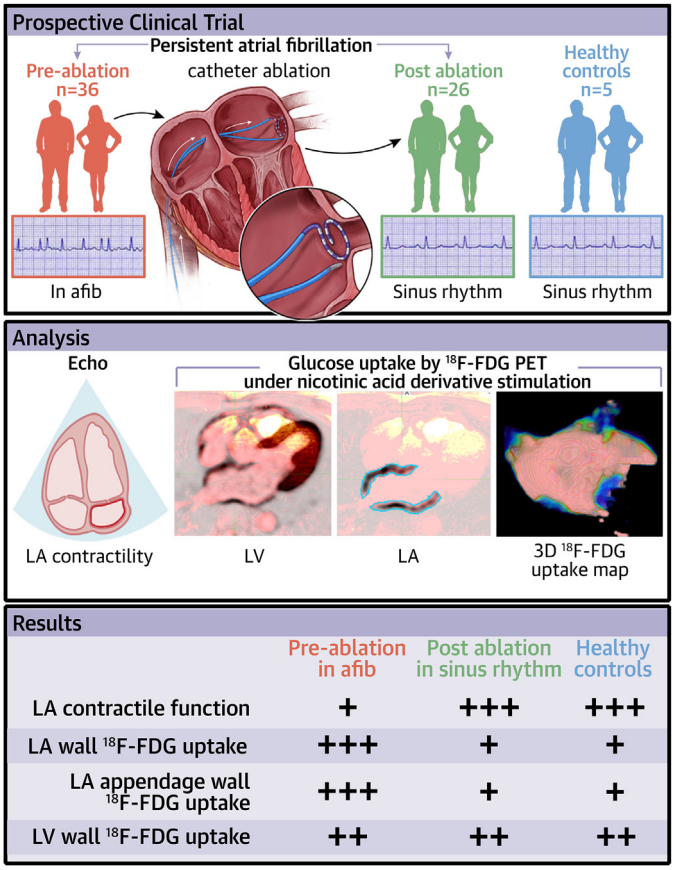

	Pre-ablation in afib	Post ablation in sinus rhythm	Healthy controls
LA contractile function	+	+++	+++
LA wall ^{18}F-FDG uptake	+++	+	+
LA appendage wall ^{18}F-FDG uptake	+++	+	+
LV wall ^{18}F-FDG uptake	++	++	++

Marchandise S, et al. J Am Coll Cardiol Basic Trans Science. 2023;■(■):■-■.

HIGHLIGHTS

- **AF affect atrial energy demands, resulting in metabolic stress. This metabolic imbalance increases glucose uptake and is associated with the development of LA remodeling which predicts AF persistence.**
- **Under metabolic conditions which favor glucose use by cardiomyocytes, patients with persistent AF present increased LA and LAA FDG uptake, while the FDG uptake in the LV was similar.**
- **After return to SR, under similar conditions and with similar LV FDG uptake, LA and LAA FDG uptake decreased significantly, despite improvement of LA contractile function.**
- **This suggests either higher overall myocardial metabolism and lower myocardial efficiency or metabolic shift to glucose as substrate in AF.**

ISSN 2452-302X https://doi.org/10.1016/j.jacbts.2023.11.001

ABBREVIATIONS AND ACRONYMS

2D = 2-dimensional

3D = 3-dimensional

AF = atrial fibrillation

CA = catheter ablation

cMR = cardiac magnetic resonance

EF = ejection fraction

FDG = 18-fluorodeoxyglucose

LA = left atrium

LAA = left atrial appendage

LGE = late gadolinium enhancement

LV = left ventricle

PET = positron emission tomography

ROI = region of interest

SR = sinus rhythm

SUV = standardized uptake value

SUMMARY

The role of atrial metabolism alterations for initiation and atrial fibrillation (AF) persistence remains poorly understood. Therefore, we evaluated left atrial glucose metabolism by nicotinic acid derivative stimulated 18-fluorodeoxyglucose positron emission tomography in 36 patients with persistent AF undergoing catheter ablation before and 3 months after return to sinus rhythm and compared values against healthy controls. Under identical hemodynamics and metabolic conditions, and although left ventricular FDG uptake remained unchanged, patients in persistent AF presented significantly higher total left atrial and left atrial appendage uptake, which decreased significantly after return to sinus rhythm, despite improvement of passive and active atrial contractile function. These findings support a role of altered glucose metabolism and metabolic wasting underlying the pathophysiology of persistent AF. (J Am Coll Cardiol Basic Trans Science 2023;■:■–■)

Atrial fibrillation (AF) is the most common rhythm disorder in clinical practice and its persistent form remains a challenge for the clinician. However, the mechanisms of AF initiation and/or progression to both more persistent forms, remain poorly understood. Structural and functional atrial remodeling, and particularly the development of progressive atrial fibrosis, are well-established hallmarks of AF persistence.[1] Experimental studies have also pointed to an important role of atrial metabolic deregulation in AF.[2,3] However, so far, there have been few studies evaluating atrial myocardial metabolism in patients in vivo. 18-Fluorodeoxyglucose (FDG) positron emission tomography (PET) allows for the evaluation of glucose uptake and phosphorylation in the left ventricle (LV) in various diseases[4] and could be a valuable tool for studying left atrium (LA) metabolism in AF. Indeed, through recent improvements in digital PET camera technologies, it is now also possible to quantitatively analyze the FDG uptake in the LA.[5] Although a few prior studies have described increased atrial FDG uptake in patients with AF,[6-10] this was not done under standardized metabolic conditions, which is critical, because glucose uptake is not only dependent on the rate of glucose use of the heart, but also on substrate availability. Oral administration of a nicotinic acid derivative (acipimox) inhibits peripheral lipolysis decreasing plasma levels of free fatty acids and stimulates preferential glucose use by cardiac myocytes.[11]

The objectives of the current study were, therefore, to quantitatively evaluate glucose uptake in nondiabetic patients with persistent AF under well-controlled metabolic conditions using FDG PET after nicotinic acid administration before catheter ablation (CA) and to compare them with healthy volunteers and with themselves after return to sinus rhythm (SR).

METHODS

STUDY PROTOCOL AND POPULATION. This prospective trial (TRIATLON [Atrial Perfusion - Metabolism and Fibrosis in Atrial Fibrillation]; EudraCT reference 2019-001813-17A) was approved by our internal review board (2018/17OCT/389), and written informed consent was obtained from all participants. From January 2020 to September 2022, we identified patients with symptomatic persistent AF referred to our institution for CA who met the following inclusion criteria: nondiabetic, aged 18 to 80 years, and without prior AF ablation. Exclusion criteria were: hyperthyroidism, renal failure (glomerular filtration rate of <30 mL/m^2), infiltrative, hypertrophic or other cardiomyopathies, significant valvular disease, and left atrial appendage (LAA) thrombus as identified on preoperative transesophageal echocardiography. The

From the [a]Division of Cardiology, Department of Cardiovascular Diseases, Cliniques Universitaires St. Luc, Brussels, Belgium; [b]Pôle de Recherche Cardiovasculaire (CARD), Université Catholique de Louvain, Brussels, Belgium; [c]Division of Nuclear Medicine, Cliniques Universitaires St. Luc, Brussels, Belgium; and the [d]Pole Molecular Imaging, Radiotherapy & Oncology (MIRO), Institut de Recherche Expérimentale et Clinique (IREC), Université Catholique de Louvain, Brussels, Belgium.
The authors attest they are in compliance with human studies committees and animal welfare regulations of the authors' institutions and Food and Drug Administration guidelines, including patient consent where appropriate. For more information, visit the Author Center.

Manuscript received May 25, 2023; revised manuscript received November 6, 2023, accepted November 6, 2023.

FIGURE 1 **Workflow of Segmentation and Postprocessing of Left Atrial FDG-PET Images**

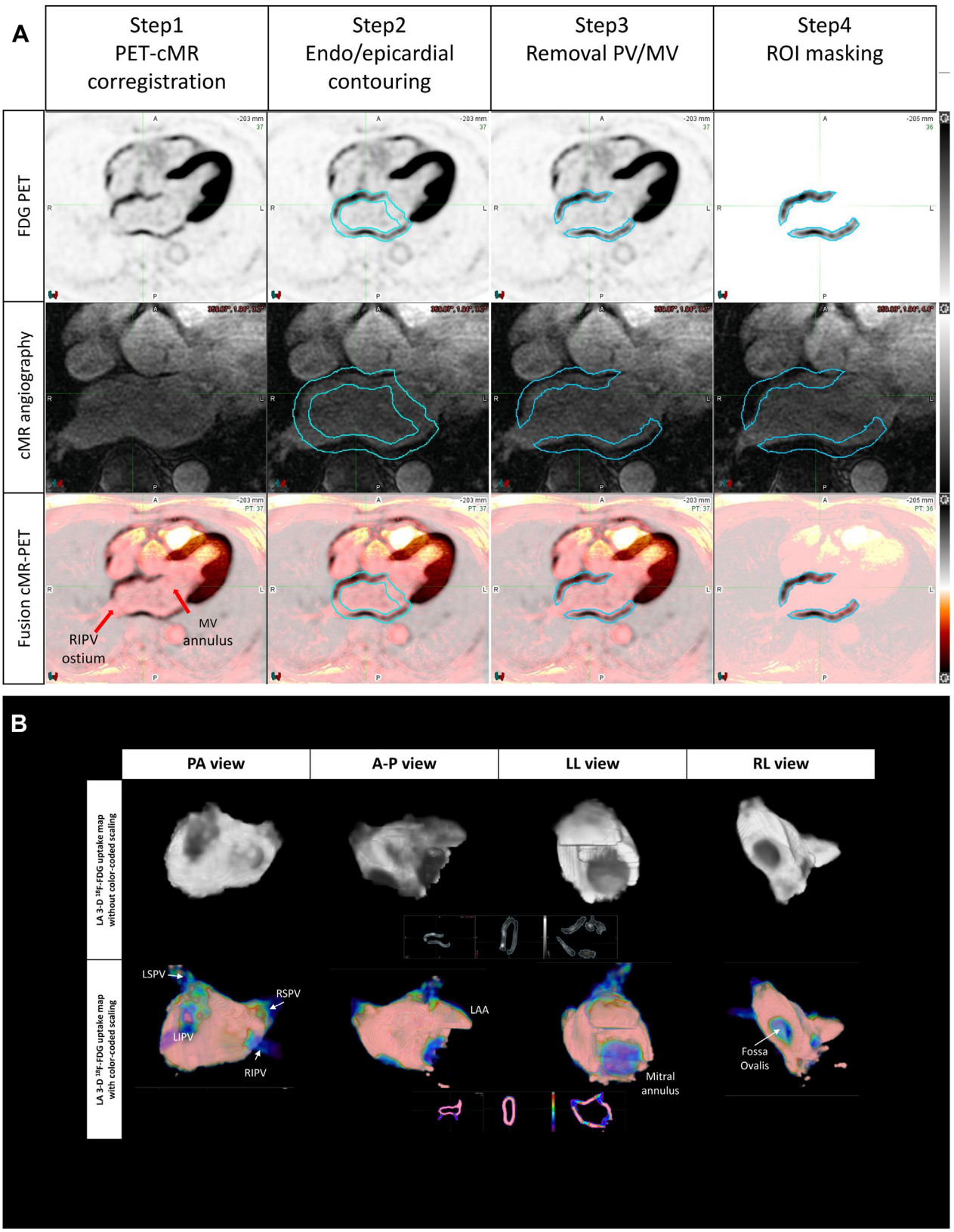

Continued on the next page

TABLE 1 Characteristics of the Study Population

Characteristics	Patients with AF (n = 36)	HV (n = 5)	*P* value
Clinical parameters			
Age (years)	64.3 ± 6.9	68.9 ± 4.8	0.114
Sex (M/F)	29/7	3/2	0.457
Weight (kg)	88.1 ± 9.6	76.0 ± 13.9	0.127
BMI (kg/m^2)	28.9 ± 3.5	24.8 ± 3.3	0.052
CV risk factors			
Hypertension	14 (38.9)	0	<0.001
Hypercholesterolemia	18 (50.0)	4 (80.0)	0.220
Diabetes	0 (0)	0 (0)	/
Family history of CAD	13 (36.1)	2 (40.0)	0.886
Smoking	11 (30.6)	0 (0.0)	<0.001
Hemodynamic and metabolic parameters			
SBP (mm Hg)	127.6 ± 10.9	129.0 ± 5.4	0.663
HR (BPM)	84.0 ± 13.5	71.0 ± 7.4	0.081
Glycemia (mg/dL)	98.8 ± 13.8	96.0 ± 6.8	0.480
Insulinemia (mIU/L)	69.5 ± 36.5	65.3 ± 3.0	0.804
eGFR (mL/min)	70.5 ± 14.5	81.0 ± 12.9	0.156
Echocardiographic parameters			
LVEF (%)	58.5 ± 9.3	64.2 ± 5.6	0.092
LA diameter (mm)	46.9 ± 5.2	38.6 ± 6.7	0.047
LA volume (mL/m^2)	59.3 ± 18.0	17.5 ± 3.5	<0.001
cMR parameters			
LVmass indexed (g/m^2)	56.9 [13.4]	46.5 [17.2]	0.202
LVEDVi (mL/m^2)	75.2 [19.2]	62.2 [14.8]	0.024
LVEF (%)	50.8 ± 8.1	56.7 ± 3.5	0.072
RVEDVi (mL/m^2)	74.8 ± 14.2	60.2 ± 19.6	0.022
RVEF (%)	51.7 ± 8.1	57.5 ± 9.1	0.145

Data are mean ± SD, number (percentage), or median (IQR).

AF = atrial fibrillation; BMI = body mass index; CAD = coronary artery disease; eGFR = estimated glomerular filtration rate; HR = heart rhythm; HV = healthy volunteers; LA = left atrium; LVEDVi = left ventricle end-diastolic volume indexed; LV = left ventricle; LVEF = left ventricular ejection fraction; RVEDVi = right ventricle end-diastolic volume indexed; RVEF = right ventricular ejection fraction; SBP = systolic blood pressure.

study protocol consisted of a nicotinic acid enhanced atrial FDG PET scan, cardiac magnetic resonance (cMR), and a transthoracic echocardiogram in AF before CA. Tests were repeated 3 to 6 months after CA in patients who had successfully returned to persistent SR for a duration of >2 months. A total of 36 patients with AF underwent baseline FDG-PET in AF and 26 patients underwent follow-up PET in SR. The study group was compared with 5 healthy, nondiabetic, age-matched controls without a history of cardiac disease or AF who underwent the same FDG PET/CT, cMR, and transthoracic echocardiogram protocol.

CARDIAC MR. Cardiac MR was acquired using a 3T system (Signa Premier, GE Healthcare). After localizer images, a 3-dimensional (3D) contrast enhanced angiographic image of the LA was acquired after injection of 0.1 mmol/kg Gd-DTPA. Then consecutive cine steady-state free precession short-axis images covering the entire heart and, respectively, 1-, 2-, 3-, and 4-chamber long-axis images were acquired. Left and right ventricular and atrial end-diastolic and end-systolic volumes and ejection fractions were computed using Medviso software (Lund Sweden). Late gadolinium images of the ventricle were acquired using 2-dimensional (2D) single shot inversion recovery images in the same prescriptions. Finally, 20 minutes after contrast injection, atrial fibrosis was evaluated by a protype ECG-triggered, free-breathing navigator gated high-resolution (1.5 × 1.5 × 1.5 mm) 3D whole heart late gadolinium enhancement (LGE) sequence (Hearty, work in progress GE Healthcare). Images were acquired with optimized trigger time in end-systole with a field of view of 400 mm, with individual adjustment of the inversion time to optimized nulling of the LA myocardium. LA wall volumes were manually segmented from the delayed-enhanced cardiac MR images using Slicer3D image processing software (version 4.11.20210226) and the Visualization toolkit library in Python 3.10. Fibrosis by LGE-cMR was evaluated using as reference 2SD of the average intensity of the enhancement around the mitral valve. AF-LGE was classified by Utah stages as I to IV as, respectively, atrial LGE of 0% to 10%, 10% to 20%, 20% to 40%, and >40% LGE.[12]

ATRIAL PET IMAGING. FDG PET/CT was performed using a high-resolution digital 64 slice PET/CT system (Vereos TOF- Philips Healthcare) using a previously optimized protocol to enable the reconstruction of high-resolution atrial PET images.[5] Patients were studied after overnight fasting and received a nicotinic acid derivative (acipimox 250 mg) to maximally stimulate myocardial glucose uptake. Before tracer injection levels of fasting glucose, insulin, and free fatty acids were measured in venous blood samples. Images were acquired 90 minutes after injection of 300 mBq of FDG using a 10-minute nongated CT attenuation-corrected scan (voxel size, 2 mm using

FIGURE 1 Continued

(A) PET images were co-registered with cMR angiographic images. Then a mask of the inner and outer contours of the LA was manually defined on cMR angiographic images, pulmonary veins and mitral valve were cut and the mask was copied to the PET images. This allowed definition of a 3D ROI of the FDG uptake of the LA wall. (B) Rendered 3D volumetric model of the left atrium, before (top) and after (bottom) color coded for maximum FDG SUV intensity from different views. cMR = cardiac magnetic resonance; FDG-PET = 18-fluorodesoxyglucose positron emission tomography; LA = left atrial; LAA = left atrial appendage; LIPV = left inferior pulmonary vein; LSPV = left superior pulmonary vein; MV = mitral valve; RIPV = right inferior pulmonary vein; ROI = region; RSPV = right superior pulmonary vein of interest.

standard manufacturer ordered subsets maximization expectation algorithms) and were reconstructed using a 3D ordered-subset expectation maximization algorithm (15 subsets, 4 iterations).

Quantitative measurements of glucose uptake were performed using MIM software (MIM Encore version 7.1.3, MIM Software Inc.). PET images were co-registered with contrast enhanced angiographic cMR images and using 3D multiplanar view, the atrial wall was segmented by tracing the epicardial and endocardial contours of the atrium, excluding pulmonary vein ostia and mitral valve annulus (Figure 1A). A mask of the area including these 2 contours was achieved and allows the construction of a 3D region of interest (ROI) representing a 3D glucose uptake mapping of the LA wall (Figure 1B). Additional ROIs were placed on the LAA, LV, and blood pool (for background correction). Atrial glucose standardized uptake value (SUV) was measured within each ROI as tracer activity (MBq/mL)/injected dose per patient body weight (MBq/kg) after correcting for decay. For each ROI, the maximum, minimum, mean, and total SUV were measured. The target to background ratio was computed for each of LV LA and LAA ROIs as the ratio of the ROI SUVmean to the SUVmean of the cavity blood pool (background). Finally, we also computed the mean LA to LV SUV ratio. Inter- and intra-observer reproducibility of measurements were assessed in 3 regions of interest by 2 operators (SM and QG) in 10 randomly selected patients.

TRANSTHORACIC ECHOCARDIOGRAPHY. We acquired 2D transthoracic echocardiograms using an EPIC sonography system and stored on a Intellispace PACS system (both Philips Healthcare). Images were analyzed offline by 1 observer (SM) and all measurements were performed by averaging 3 cardiac cycles as described previously.[13] LV volumes and ejection fraction were calculated using Simpson's biplane method. The E/e′ ratio was calculated from peak mitral flow E and the average of septal and lateral e′ tissue Doppler velocities. LA volume and strain analysis were performed on dedicated apical 4- and 2-chamber views of the LA acquired with a frame rate between 60 and 80 frames per second and analyzed using Image-Arena cv4.6 (TomTec Imaging Systems) in duplicate by 2 experienced blinded echocardiographers (SM and QG). Maximal and minimal indexed LA volumes were measured, respectively, at the end of LV systole and LV diastole and indexed to body surface area. Fractional area change and ejection fraction of passive emptying fraction were computed respectively, as the percentage ratio of change of LA area and volume during systole. We also computed Reservoir Global Peak Atrial Longitudinal Strain conduit and contraction phase strains. All strains were computed using LV end-diastole as the zero-strain point. The left atrial strain contraction was only computed when patients had returned to SR.

TABLE 2 Atrial Function and Metabolism in Persistent AF vs HV

	Persistent AF (n = 36)	HV (n = 5)	*P* Value
FAC (%)	13.8 ± 6.1	37.0 ± 5.4	<0.001
LAEF (%)	19.8 ± 8.2	47.7 ± 7.7	0.004
GPALS (%)	8.8 ± 3.5	28.3 ± 4.9	<0.001
LV SUV mean	11.4 ± 5.1	14.6 ± 3.5	0.115
LA SUV mean	2.9 ± 0.8	2.6 ± 0.3	0.151
LA/LV ratio	0.3 ± 0.2	0.2 ± 0.0	0.002
LAA SUV mean	3.5 ± 1.1	2.5 ± 0.4	0.011
LAA/LV ratio	0.4 ± 0.2	0.2 ± 0.0	<0.001

Data are mean ± SD. *P* value expresses the difference between HV and patients with persistent patient during AF.

FAC = fractional area change; LAEF = left atrial ejection fraction; GPALS = global peak atrial longitudinal strain; LAA = left atrial appendage; SUV = standardized uptake value; other abbreviations as in Table 1.

ELECTROANATOMICAL MAPPING AND CA PROCEDURE. Electroanatomic mapping of the LA was obtained using the ConfiDENSE CARTO3 system v6.0.70 using the 2515 Variable Loop Lasso Multi-Electrode Eco Nav (Biosense Webster) using ≥1,000 measurements as described previously.[13] Electrical cardioversion was attempted after an initial mapping, and mapping was repeated in SR. Low voltage area was defined as bipolar peak-to-peak voltage amplitude of <0.5 mV in SR and <0.31 mV in AF. All patients underwent radiofrequency PVI with additional lines or complex atrial fractionated electrogram ablations performed at the physician's discretion.

STATISTICAL ANALYSES. All analyses were performed using SPSS version 26.0 (SPSS, Inc) and R software version 3.5 (The R Project) and a *P* value of <0.05 was considered statistically significant. Our study had 80% power with 26 patients to demonstrate a mean SUV change of 0.78 ± 1.03 between baseline and follow-up using a paired *t*-test and to demonstrate a mean SUV difference of 0.55 ± 0.80 between 36 patients with AF and 5 controls using an unpaired *t*-test. Continuous values were evaluated for normality using QQ plots, histograms, and the Kolmogorov-Smirnov test, and are expressed as the mean ± SD or the median with IQR, depending on their distribution. These values were then compared between patients and controls, respectively, using the 2-sided *t*-test or the Mann-Whitney *U* test, whereas individual data in patients before and after return to SR were compared either with the paired *t*-test or the Wilcoxon signed-rank test. Categorical data are expressed as counts and percentages and

FIGURE 2 Difference in FDG Uptake Parameters Between Persistent Atrial Fibrillation Patients, 3 Months After SR Restore and Healthy Volunteers in 3 ROIs

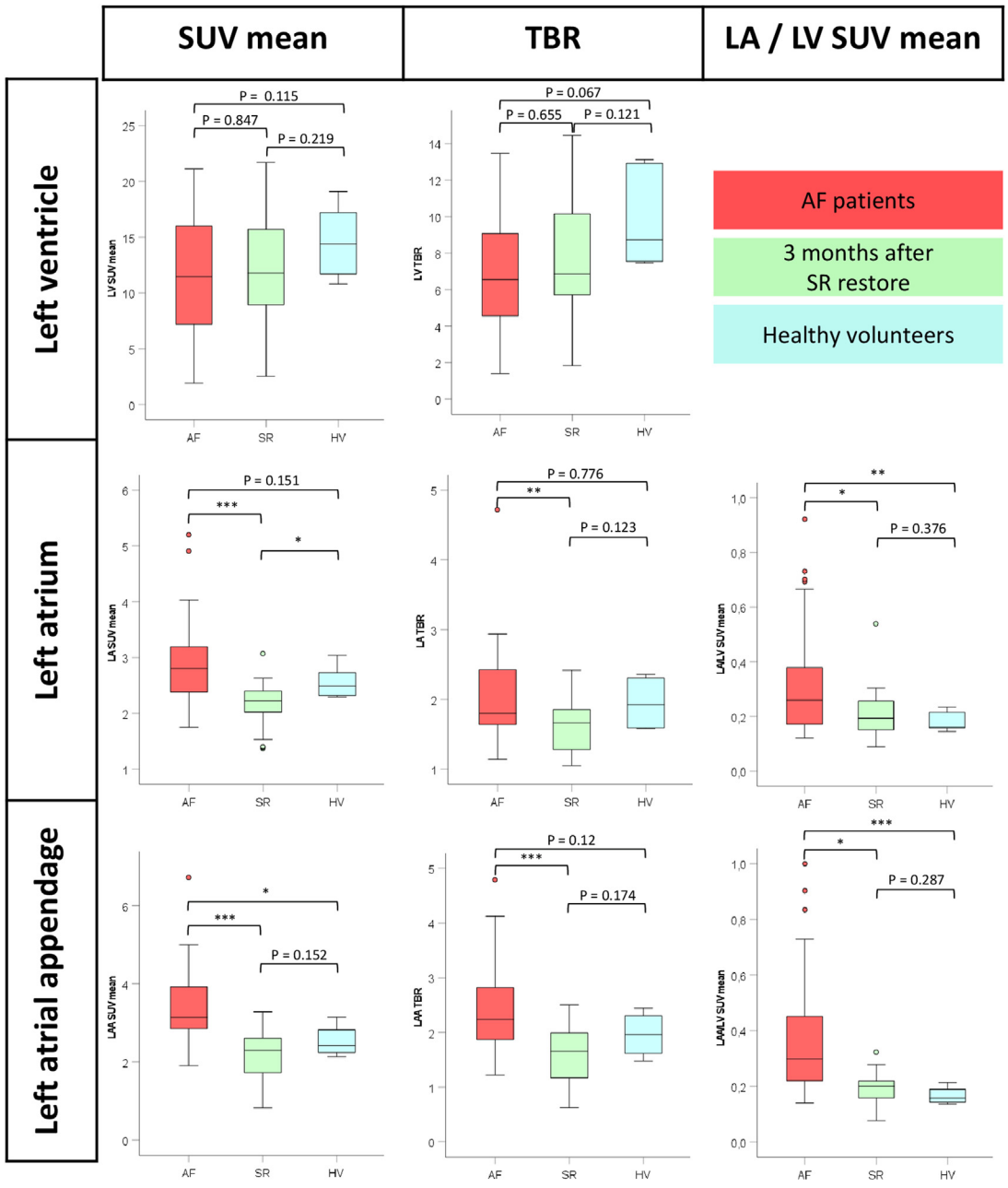

Box plot showing difference in mean standardized uptake value (SUV), target to background ratio (TBR), and LA/LV SUV mean ratio between patients with persistent atrial fibrillation (AF) 3 months after SR restore and healthy volunteers (HV) in three ROIs (left ventricle [LV], LA, and LAA). The box represents IQR, the line within the box indicates the median value, whiskers show minimum/maximum values. *$P < 0.05$, **$P < 0.01$; ***$P < 0.001$. SR = sinus rhythm; other abbreviations as in Figure 1.

were compared using the chi-squared test. The relationship between PET parameters and LVA or echocardiographic parameters was evaluated by linear regression analysis and the Pearson correlation coefficient. Intra- and interobserver reproducibility of SUV measurements was analyzed using the coefficient of variation and intraclass correlation coefficient with 95% CIs for agreement.

RESULTS

PATIENT CHARACTERISTICS. Table 1 presents the baseline characteristics of the patients with AF and healthy volunteers. The patients with AF were predominantly male (n = 29 [80.6%]) with an average age of 64.3 ± 6.9 years and the average duration of AF since first diagnosis was 4.7 ± 4.0 years. Nineteen patients (52.7%) patients had AF persisting >6 months and 8 (22.2%) >1 year. The median European Heart Rhythm Association score was 2 (IQR, 1) and the median CHADS-VASC score was 2 (IQR, 2). Three patients (15.0%) had a history of congestive heart failure and 5 (13.8%) had had a transient ischemic attack, stroke, or thromboembolic event. Seven patients (19.4%) had coronary artery disease and 4 had suffered from a myocardial infarction. In terms of medical treatment 24 patients (66.7%) were treated with beta-blockers, 3 (8.3%) received sotalol, 9 (25.0%) amiodarone, and 6 (16.7%) a class I antiarrhythmic drug. All but 1 patient received direct oral anticoagulation. Ten patients (27.8%) received statins. No patient was treated with metformin or other antidiabetic drugs.

No statistically significant discrepancies were observed between patients with AF and healthy volunteers in terms of sex, age, and weight. The patients exhibited a tendency for higher body mass index than controls, along with a significantly greater prevalence of cardiovascular risk factors (eg, hypertension and smoking). At the time of the study, systolic blood pressure, estimated glomerular filtration rate, glycemia, and insulinemia did not differ significantly between patients and controls. Notably, no patient had hyperglycemia >110 mg/dL. All patients with AF had adequate control of resting heart rate (<110 bpm); nevertheless, heart rate was slightly but significantly higher in patients than in controls. Echocardiographic and cMR left, and right ventricular volumes and ejection fraction was similar, but the LA diameter and volume was higher in patients with AF than in controls. No patient had LGE in the myocardium or any indication for infiltrative disease (amyloidosis/sarcoidosis). The average atrial LGE extent was 11.7 ± 9.5% (range, 0.0%-45.1%). Nine patients were considered to have Utah stage I, 19 Utah stage II and the remaining 6 patients presented with extensive atrial fibrosis (Utah stage III or IV). After PVI ablation, LGE was nonsignificantly different (14.3 ± 8.8%; $P = 0.273$). By electroanatomical mapping, the low-voltage area represented 7.4 ± 6.8% of the entire atrium.

TABLE 3 Hemodynamics, Atrial Function, and Metabolism in Persistent AF After Return to SR and in HVs

	Persistent AF (n = 26)	SR (n = 26)	HV (n = 5)	*P* value (AF vs SR)	*P* value (SR vs HV)
HR (bpm)	80.9 ± 17.6	62.3 ± 10.5	71.0 ± 7.4	<0.001	0.056
SBP (mm Hg)	126.4 ± 10.6	130.6 ± 7.9	129 ± 5.4	0.205	0.634
Glycemia (mg/dL)	97.6 ± 13.9	92.8 ± 9.3	96.0 ± 6.8	0.070	0.394
Insulinemia (mIU/L)	59.6 ± 39.9	69.2 ± 43.5	65.3 ± 3.0	0.605	0.783
FFA (mg/dL)	142.0 ± 41.1	120.9 ± 52.7	NA	0.419	NA
LVEF (%)	59.6 ± 9.5	54.8 ± 2.2	64.2 ± 5.6	0.664	0.136
LV aGLS	NA	15.5 ± 0.7	18.1 ± 0.5	NA	<0.001
E wave velocity (cm/s)	75.5 ± 20.0	62.4 ± 21.4	65.4 ± 13.9	0.028	<0.001
A wave velocity (cm/s)	NA	58.2 ± 9.8	75.4 ± 18.2	NA	<0.001
Average e′ (cm/s)	9.6 ± 2.9	7.8 ± 1.8	7.1 ± 0.7	<0.001	0.022
E/e′ (%)	8.9 ± 3.8	8.1 ± 2.7	9.2 ± 1.6	0.241	0.141
FAC (%)	13.9 ± 6.2	25.4 ± 6.8	37.0 ± 5.4	<0.001	0.004
LAEF (%)	19.9 ± 8.4	33.5 ± 9.3	47.7 ± 7.7	<0.001	0.001
LASct (%)	NA	7.3 ± 3.0	15.2 ± 4.1	NA	0.001
LAScd (%)	NA	10.2 ± 5.1	13.1 ± 2.1	NA	0.045
LASr (%)	8.8 ± 3.5	17.3 ± 2.2	28.3 ± 4.9	<0.001	0.003
LV SUV mean	11.1 ± 5.6	12.2 ± 4.7	14.6 ± 3.5	0.847	0.668
LA SUV mean	2.9 ± 0.9	2.2 ± 0.4	2.6 ± 0.3	<0.001	0.035
LA/LV ratio	0.4 ± 0.2	0.2 ± 0.1	0.2 ± 0.0	0.018	0.339
LAA SUV mean	3.2 ± 1.1	2.1 ± 0.6	2.5 ± 0.4	<0.001	0118
LAA/LV ratio	0.4 ± 0.3	0.2 ± 0.1	0.2 ± 0.0	0.001	0.306

Data are ± SD.

FFA = free fatty acid; LAScd = left atrial strain conduit; LASct = left atrial strain contraction; LASr = left atrial strain reservoir; NA = not applicable; other abbreviations as in Tables 1 and 2.

ATRIAL FUNCTION AND FDG UPTAKE IN PATIENTS DURING PERMANENT AF VS CONTROLS. Table 2 summarizes data on atrial function and FDG uptake in patients with AF and in healthy volunteers. As expected, atrial functional parameters (fractional area change, EF, and LA strains) were significantly lower in patients with persistent AF than in controls. The F18 dose injected (7.9 ± 0.5 mCi vs 7.7 ± 0.5 mCi; $P = 0.974$), the delay to acquisition (96.9 ± 9.2 vs 96.0 ± 5.6 min; $P = 0.126$), and the acquisition duration (10.4 ± 1.8 vs 10.0 ± 0.1; $P = 0.183$) were similar among patients and controls. The image quality was high in all but 1 examination, likely owing to an issue with the injection. This factor enabled accurate identification of all the atrial segments, including the LAA in 97.2% of examinations. Although the FDG uptake was similar in the LV wall in patients with AF as in healthy controls, patients with AF had significantly higher FDG uptake in the LA wall and particularly in the LAA than controls. Hence the ratio of mean SUV of the LA to LV and LAA to LV was significantly higher in AF than in controls (Figure 2).

FIGURE 3 Individual Evolution of LA FDG Uptake and Atrial Contractile Function Between Persistent AF and After SR Restore

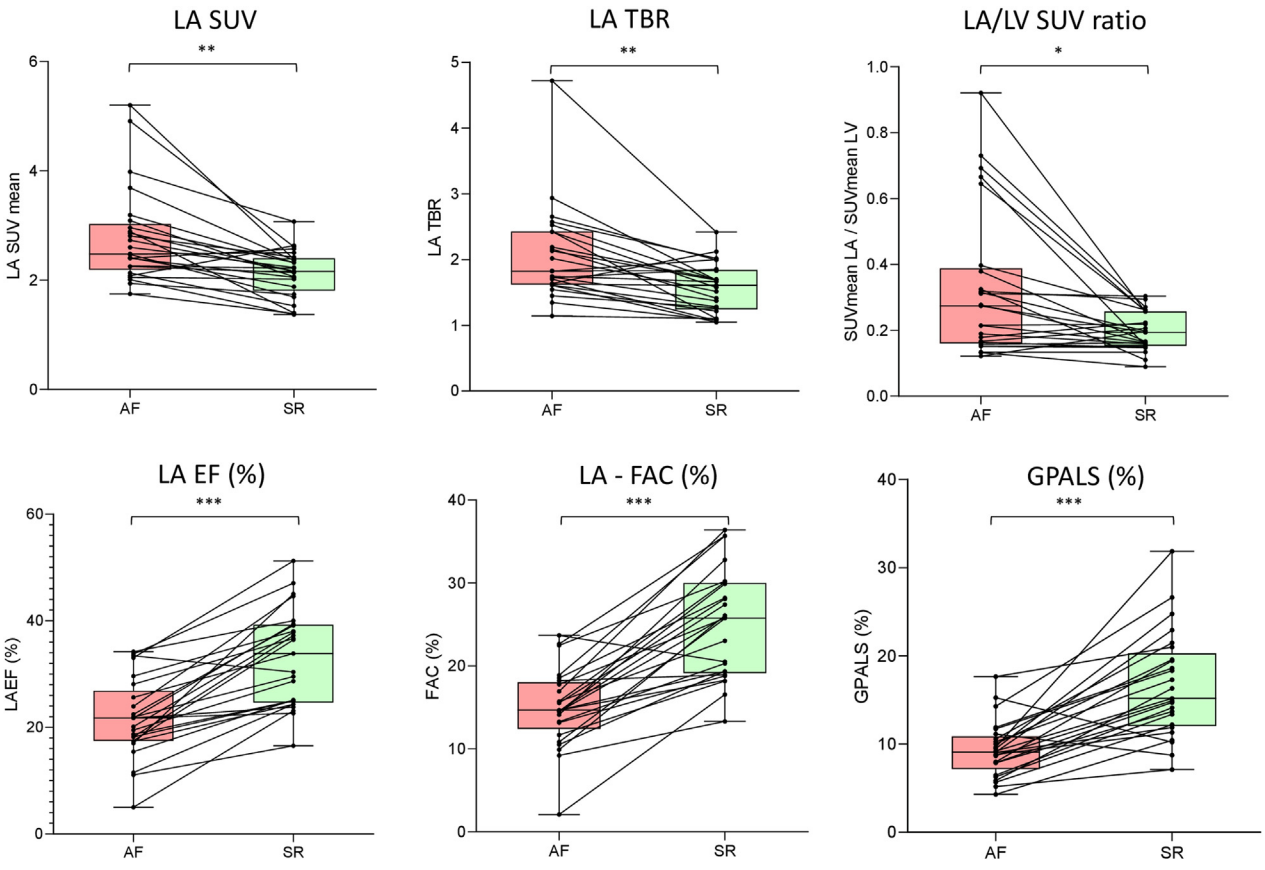

Spaghetti plots showing the difference of LA FDG uptake (top) and atrial contractile function (bottom) between persistent AF and restoration of SR. Lines connect symbols for each subject and represent individual variation of FDG uptake or echocardiographic parameters. The box represents IQR, the line within the box indicates the median value, whiskers show minimum/maximum values. AF = atrial fibrillation; FAC = fractional area change; FDG = fluorodeoxyglucose; GPALS = global peak atrial longitudinal strain; LAEF = left atrial ejection fraction; LV = left ventricle; other abbreviations as in Figures 1 and 2. *$P < 0.05$, **$P < 0.01$; ***$P < 0.001$.

CHANGES OF FDG UPTAKE AND CONTRACTILE FUNCTION AFTER RETURN TO SR. All patients successfully underwent CA. CA consisted of PV ablation in all patients and additional lines or complex atrial fractionated electrogram ablations in 8 patients (22.2%). The data from the 26 patients undergoing repeat FDG PET post-ablation are shown in Table 3 and in Figure 3. The repeat exam was performed on average 4.4 ± 1.8 months (range, 3-8 months) after CA and return to SR. All patients were in SR for >2 months at the time of the repeat examination. A significant increase was not observed in cMR LGE in LA after ablation, except for the lesions in ostia of the pulmonary veins, which were not included in PET ROI measurements. Hemodynamics and metabolic conditions were not significantly different in SR as compared with persistent AF, except for heart rate, which was slightly lower in SR than in persistent AF. The LVEF was higher in the control group. This difference was weak, although the LV strain was significantly better. There were also no differences in injected FDG dose injection (7.9 ± 0.5 mCi vs 7.9 ± 0.5 mCi; $P = 0.974$), delay to acquisition (98.1 ± 9. min 6 vs 95.2 ± 7.9 min; $P = 0.228$) and the acquisition duration (10.6 ± 2.1 vs 10.0 ± 1.0; $P = 0.185$). Also, patient treatment was not significantly different especially for beta-blockers ($P = 0.327$) and angiotensin receptor blockers or angiotensin-converting enzyme inhibitors ($P = 0.161$).

An example of a typical PET study of a patient in persistent AF and after return to SR is shown in Figure 4, an the individual changes of LA contractile function and FDG uptake SUV in LA are shown in Figure 3. Patients significantly improved passive (fractional area change, left atrial ejection fraction, and left atrial strain reservoir) and regained active

FIGURE 4 Reduction of Atrial FDG Uptake in a Patient During Persistent AF and 3 Months After SR Restore

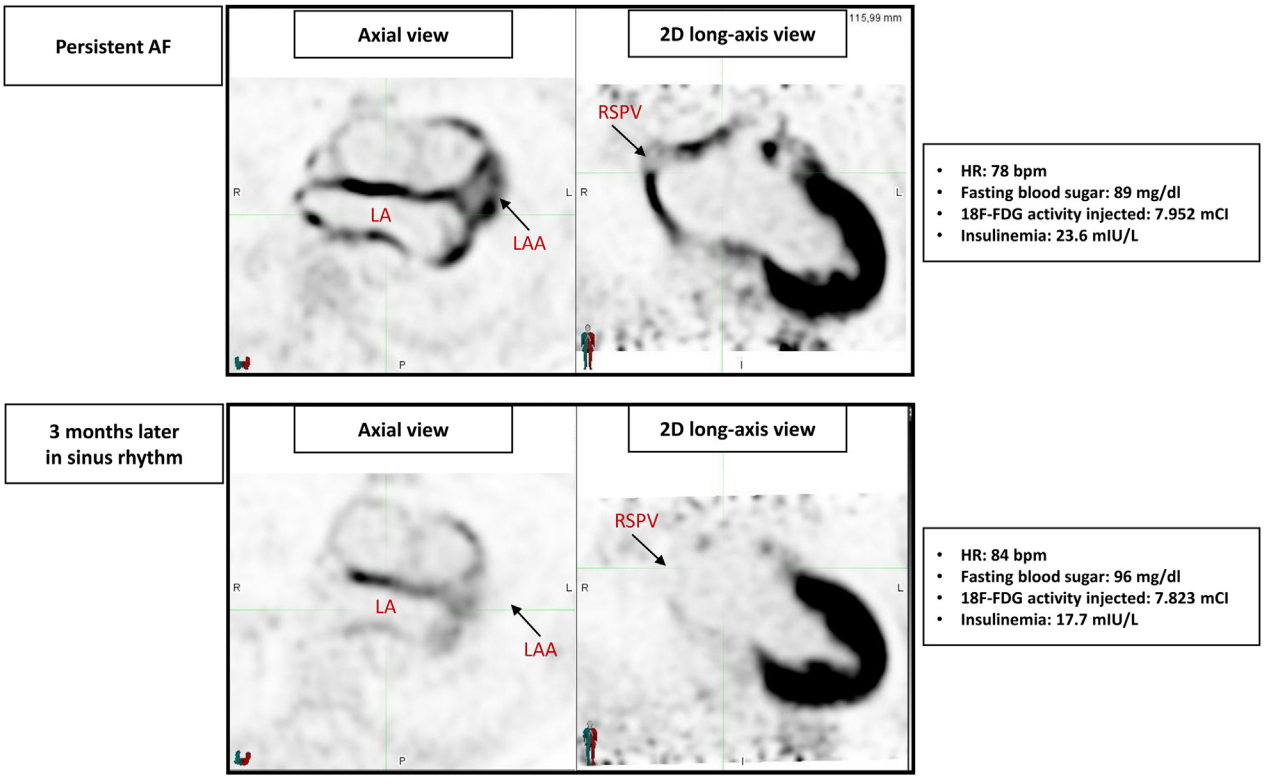

Patient preparation and metabolic conditions and image analysis and postprocessing were identical. Abbreviations as in Figures 1 and 2.

atrial function (A wave velocity and left atrial strain contraction), which was previously absent. This occurred while on average the mean SUV FDG uptake in LA and LAA decreased respectively by 20.4% and 34.1%, and in the absence of significant change in mean SUV uptake in the LV. Therefore, the average LA/LV and LAA/LV FDG uptake also significantly decreased. The decrease of LA FDG uptake was present in all patients, but we could not observe direct relation to an LA low-voltage area or LGE. However, despite a decrease in FDG uptake in patients in SR, relative atrial FDG uptake (mean LA to LV SUV ratio) remained slightly higher than that of volunteers, although the absolute atrial uptake value was nonsignificantly lower. Figure 5 and 6 show examples of 3D FDG uptake maps of the LA and corresponding electroanatomical maps. Homogenous FDG uptake as observed in most patients, correlated with normal electroanatomical maps (Figure 5), whereas areas of decreased FDG uptake spatially accorded with areas of low electrical voltage and scarring (Figure 6).

REPRODUCIBILITY OF MEASUREMENTS. Intra- and interobserver variability analysis of SUV measurements in LA, LAA and LV found the reproducibility was high with intraclass correlation coefficient measures ranging from 0.87 to 0.99, as detailed in Table 4.

DISCUSSION

The principal findings of our present study can be summarized as follows:

1) Under metabolic conditions, which favor glucose use by myocytes, patients with persistent AF present with increased relative LA/LV ratio and especially increased LAA and LAA/LV FDG uptake as compared with healthy controls.
2) After return to SR, under similar conditions and with similar LV FDG uptake, LA and LAA FDG uptake decreased significantly, despite improvement of LA contractile function.

A better understanding the pathophysiology of persistent AF is important owing to the heightened

FIGURE 5 **Representative 3D FDG Uptake Mapping in a Patient Without Electrical LA Remodeling**

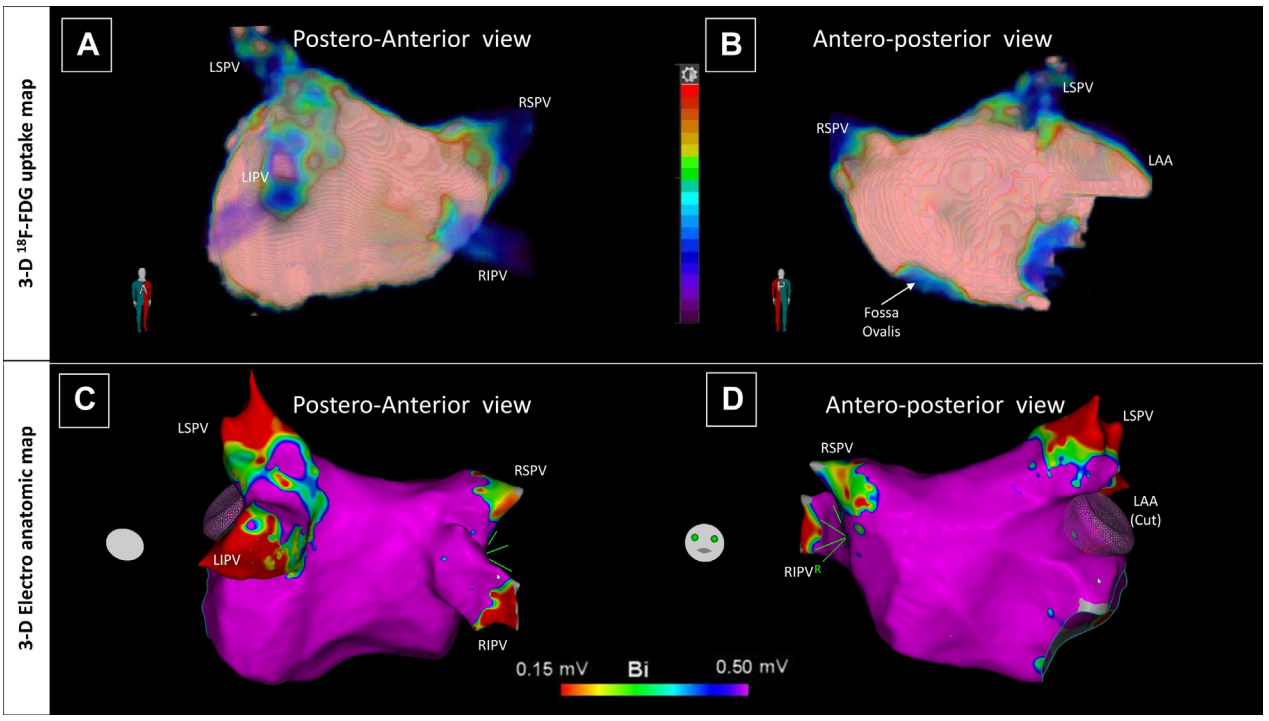

FDG-PET rendered LA model in posterior-anterior (A) and antero-posterior (B) views show homogeneous distribution of the tracer. Corresponding 3D electroanatomic maps during AF (C) and (D) shows electrically normal atrial tissue without low voltage area (purple color). Abbreviations as in Figure 1.

risk of cardiovascular morbidity and mortality associated with the condition. PET offers an ideal means of assessing myocardial metabolism in vivo. Recent improvements in PET technology have enabled higher spatial resolution and improved image quality, thereby allowing for the acquisition of high-quality PET images of the atria without influence of partial volume effect.[5] Our study is novel in that it prospectively used this technique to explore the metabolic changes in the atria of patients with persistent AF in comparison with those with restored SR. Although some previous studies have reported increased FDG uptake in atria of patients with AF,[6-10] the type of AF (ie, paroxysmal vs persistent varied); importantly, these studies were not performed under well-standardized metabolic conditions, but usually only after fasting. Indeed, considering the metabolic conditions is primordial when interpreting FDG uptake of the heart and surrounding tissues, because myocardial metabolism preference is heavily reliant on substrate availability. Therefore, the interpretation of the increased FDG signal in earlier work was complicated. Generally, increased FDG uptake has been attributed to the presence of inflammatory cells, such as macrophages and lymphocytes, in the myocardium or in adjacent epicardial adipose tissue, or both.[7] The unique and significant contribution of our study is the evaluation of a uniform cohort of nondiabetic patients with persistent AF after the administration of a nicotinic acid derivative. Nicotinic acid significantly inhibits lipolysis, thereby decreasing plasma free fatty acid concentrations and favoring glucose use by myocytes. This approach enabled us to acquire high-quality 3D PET images in both patients and controls. Furthermore, co-registration with cMR angiographic images allowed for addressing partial volume effects and enabled accurate localization of FDG uptake to the atrial wall, the fossa ovalis, mitral annulus, pulmonary vein ostia, and, importantly, the intra-atrial septum and LAA. Because these latter structures are not encircled by fatty tissue, this finding strongly suggests that FDG uptake originated from the atrial myocardium, rather than epicardial fat. Moreover, FDG uptake was also detected in healthy subjects without AF, albeit at slightly lower levels, and was found to be relatively homogeneous throughout the atria without any indication of focal uptake, suggesting that

FIGURE 6 **A 3D FDG Uptake Mapping Example in a Patient With LA Electrical Remodeling**

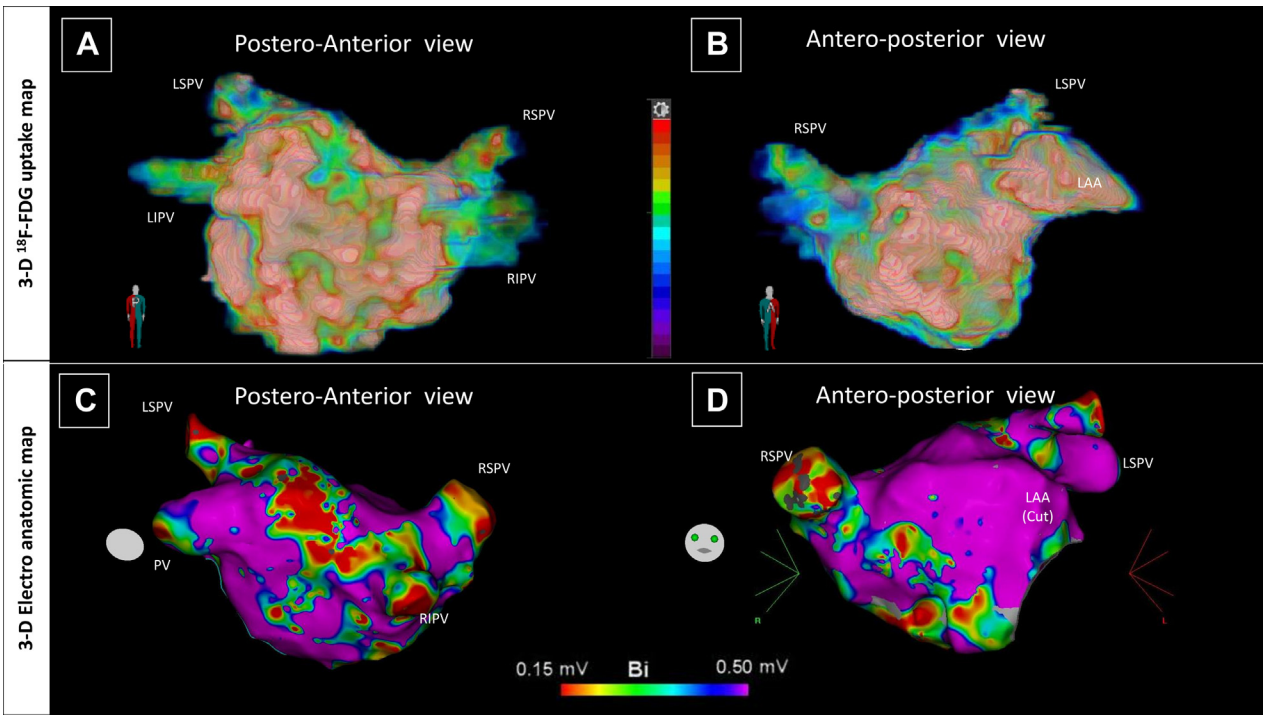

FDG-PET-rendered LA model in posterior-anterior (A) and antero-posterior (B) views show heterogeneous distribution of the tracer of the LA with low FDG uptake areas (green). Corresponding 3D electroanatomic maps (C) and (D) show low voltage area (green/red) in similar areas. Abbreviations as in Figure 1.

inflammation is unlikely to be involved, which is consistent with other reports.[9] Intriguingly, uptake in the LAA was higher than in the remaining LA, potentially indicating the greater vulnerability of the LAA to AF. Although we cannot definitively rule out an inflammatory contribution, we thus believe that the increased FDG signal observed in our study likely originated from atrial myocytes. Changes in myocardial FDG uptake could potentially also be attributed to hemodynamic and pharmacological factors, such as antiarrhythmic drugs or beta-blockers. However, no discernible changes in these factors were observed before and after the reversion to SR. Furthermore, no significant differences in FDG uptake in the LV were observed between AF after the return to SR. Therefore, we do not believe that these factors are responsible for the alterations in atrial FDG uptake that transpired after the reversion to SR. We also conducted a comprehensive multimodality evaluation of atrial structure and function, by LGE cMR and electroanatomical voltage mapping, which revealed that, despite prolonged persistent AF, most of the atrial tissue was still largely viable and not infarcted. This result was further corroborated by speckle tracking echocardiography, which demonstrated a return to mechanical activity after restoration of SR. Because CA only resulted in minimal scarring increase, mainly in the pulmonary veins, which were excluded from PET ROIs and because the SUV decreased also strongly in the LAA, which was not approached during CA, we do not believe that an increase in atrial scarring could have contributed to decrease in FDG uptake after return to SR.

We, thus, believe that our results are most consistent with either atrial metabolic wasting and overall increase of atrial oxidative metabolism, or with a metabolic shift to the preferred glucose use in atrial myocytes during persistent AF, which normalized in SR. Both could be implicated directly in the pathophysiology of the disease. Indeed, AF is characterized by the continuous, irregular, and rapid electrical activity of multiple wavelets of electrical reentry in the atria, resulting in increased rates of action potential depolarization, ion flux, and myocellular calcium overload of the atrial myocytes with enhanced rates of activation of myofilaments,[14] which are, however, mechanically inefficient. The increased myocardial workload caused by the persistent contraction of the

TABLE 4 Intraobserver and Interobserver Variability Analysis

	Intraobserver		Interobserver	
	CV	ICC	CV	ICC
LA SUV	1.3 ± 3.6	0.98 [0.95-0.99]	1.2 ± 2.3	0.97 [0.75-0.99]
LAA SUV	-8.1 ± 32.9	0.96 [0.86-0.99]	5.0 ± 7.8	0.87 [0.71-0.99]
LV SUV	-0.8 ± 6.6	0.98 [0.93-0.99]	9.2 ± 4.1	0.99 [0.88-0.99]

CV is presented as a percentage (mean ± SD) and ICC with 95% CI.

CV = coefficient of variation; ICC = intraclass correlation coefficient; other abbreviations as in Tables 1 and 2.

cardiomyocytes can lead to increased energetic demands in AF.[15] Additionally, evidence suggests that the chaotic atrial activity of AF affects the normal metabolic pathways of the myocardium, modify glucose transporter trafficking, leading to changes in the use of substrates for energy production to sustain the increased energy consumption due to the heightened workload and maintenance of the arrhythmia. This result is suggested by animal models showing that oxidative stress experienced during AF may lead to alterations of mitochondrial function,[16] and that AF may result in decreased adenosine triphosphate synthesis and a metabolic shift from fatty acid beta-oxidation to glucose uptake, increased anaerobic glycolysis and lactic acid production, adenosine monophosphate-activated protein kinase activation, changes in Glucose transporter expression, glucose transporters trafficking, and structural remodeling of the atrium,[17] with increased glycogen accumulation and reduced myofilaments, mimicking those observed in ventricular myocytes from chronic hibernating myocardium.[18] It is also supported by microarray probes showing alterations of mRNA expression transcriptome in atrial tissue[19,20] in humans. All these paradigms support the existence of an atrial cardiomyopathy[21] where altered atrial metabolism is a key component of both AF initiation and progression. Indeed, the metabolic wasting might lead to ischemia, resulting in myocyte necrosis and apoptosis and subsequent replacement of the tissue by fibrosis. To our knowledge, our study is the first study to directly support such metabolic alterations in atrial cardiomyopathy by FDG imaging in patients with persistent AF. Further work is required to even better understand the underlying mechanisms of such increased FDG uptake in AF. Ideally, to understand which mechanism (increased metabolism, tissue hypoxia, ischemia, or inflammation) is prevailing, it would have been interesting to also have FDG data in a fasted state only in the same patients; this evaluation was, however, not feasible owing to the complexity of study design and radiation exposure.

CLINICAL IMPLICATIONS. Beside providing further insights into the pathophysiology of AF, our study demonstrates the feasibility of acipimox-enhanced FDG PET for high-quality atrial imaging in vivo. This technique may be comparable with cMR LGE and other imaging techniques, potentially providing clinical applications in evaluating atrial remodeling and viability before CA.[19] FDG-PET uptake could serve as an indication of preserved atrial myocyte function, thereby demonstrating the absence of atrial fibrosis. Further research should investigate the potential usefulness of this noninvasive imaging technology in clinical practice and evaluate the correlation between FDG-PET uptake and AF structural remodeling or AF duration, to guide AF ablation strategies and predict the outcomes of pulmonary vein isolation procedures.

STUDY LIMITATIONS. This single-center study had a relatively small sample size and evaluated only semiquantitative atria FDG standard uptake values, but not quantitative glucose uptake owing to the lack of an 18F input curve. No adjustments were made for multiple testing to preserve type I error; thus, the results should be interpreted with caution. We did not perform a test-retest reproducibility of FDG SUV under acipimox in healthy volunteers, nor a second FDG study under fasted conditions alone, owing to concerns for radiation exposure. Variability in lipolysis response to nicotinic acid derivates, and associated effects such as vasodilatation and increase of myocardial perfusion, could theoretically have influenced acipimox-induced stimulated glucose uptake. The actual glucose transport rate could also differ from FDG uptake rates in the case of variability of the FDG/glucose transport rate through glucose transporters, known as the so-called lumped constant. In addition, we were unable to differentiate between atrial glucose and total oxidative metabolism, which would require dynamic 11-C acetate PET imaging.

CONCLUSIONS

Using nicotinic acid–stimulated PET, we observed significantly increased FDG uptake in the LA wall during persistent AF relative to healthy controls, which significantly normalized after return to SR. These results indicate augmented glucose and overall atrial myocardial metabolism, as well as reduced atrial contractile efficiency and energy wasting in persistent AF compared with SR. These findings suggest that metabolic changes may be implicated in the perpetuation and development of persistent AF.

FUNDING SUPPORT AND AUTHOR DISCLOSURES

Grant support by the Fonds pour la Chirurgie Cardiaque de l'Université Libre de Bruxelles and by an unrestricted grant by Pfizer and Daiichi Sankyo to the cardiology division. Dr Gerber has received the grant support from the La Chirurgie Cardiaque de l'Universite Libre de Bruxelles. The other authors have reported that they have no relationships relevant to the contents of this paper to disclose.

ADDRESS FOR CORRESPONDENCE: Dr Bernhard L. Gerber, Division of Cardiology, Department of Cardiovascular Diseases, Cliniques Universitaires St. Luc UCL, Avenue Hippocrate 10 / 2806, B-1200 Woluwe St. Lambert, Belgium. E-mail: Bernhard.gerber@uclouvain.be.

PERSPECTIVES

COMPETENCIES IN MEDICAL KNOWLEDGE: Nicotinic acid–stimulated PET showed increased FDG uptake in patients with persistent AF relative to healthy controls, which normalized after return to SR. These findings support either metabolic shift or overall oxidative wasting in persistent AF.

TRANSLATIONAL OUTLOOK: Further studies using PET will allow us to better understand the metabolic alterations underlying AF and atrial cardiomyopathy. Furthermore, FDG-PET might have value to noninvasively detect atrial viability before ablation treatment.

REFERENCES

1. Nattel S, Harada M. Atrial remodeling and atrial fibrillation: recent advances and translational perspectives. *J Am Coll Cardiol*. 2014;63:2335-2345.

2. Heijman J, Dobrev D. Irregular rhythm and atrial metabolism are key for the evolution of proarrhythmic atrial remodeling in atrial fibrillation. *Basic Res Cardiol*. 2015;110:41.

3. Ghezelbash S, Molina CE, Dobrev D. Altered atrial metabolism: an underappreciated contributor to the initiation and progression of atrial fibrillation. *J Am Heart Assoc*. 2015;4:e001808.

4. Taegtmeyer H. Tracing cardiac metabolism in vivo: one substrate at a time. *J Nucl Med*. 2010;51(Suppl 1):80s-87s.

5. Hesse M, Marchandise S, Gerber B, Roelants V. Cardiac atrial metabolism quantitative assessment with analog and digital time of flight-PET/computed tomography. *Nucl Med Commun*. 2023;44:646-652.

6. Watanabe E, Miyagawa M, Uetani T, et al. Positron emission tomography/computed tomography detection of increased (18)F-fluorodeoxyglucose uptake in the cardiac atria of patients with atrial fibrillation. *Int J Cardiol*. 2019;283:171-177.

7. Xie B, Chen BX, Nanna M, et al. 18F-fluorodeoxyglucose positron emission tomography/computed tomography imaging in atrial fibrillation: a pilot prospective study. *Eur Heart J Cardiovasc Imaging*. 2021;23:102-112.

8. Santi ND, Wu KY, Redpath CJ, et al. Metabolic activity of the left and right atria are differentially altered in patients with atrial fibrillation and LV dysfunction. *J Nucl Cardiol*. 2022;29:2824-2836.

9. Lange PS, Avramovic N, Frommeyer G, et al. Routine (18)F-FDG PET/CT does not detect inflammation in the left atrium in patients with atrial fibrillation. *Int J Cardiovasc Imaging*. 2017;33:1271-1276.

10. Fujii H, Ide M, Yasuda S, Takahashi W, Shohtsu A, Kubo A. Increased FDG uptake in the wall of the right atrium in people who participated in a cancer screening program with whole-body PET. *Ann Nucl Med*. 1999;13:55-59.

11. Knuuti MJ, Yki-Järvinen H, Voipio-Pulkki LM, et al. Enhancement of myocardial [fluorine-18] fluorodeoxyglucose uptake by a nicotinic acid derivative. *J Nucl Med*. 1994;35:989-998.

12. Marrouche NF, Wilber D, Hindricks G, et al. Association of atrial tissue fibrosis identified by delayed enhancement MRI and atrial fibrillation catheter ablation: the DECAAF study. *JAMA*. 2014;311:498-506.

13. Marchandise S, Garnir Q, Scavee C, et al. Prediction of left atrial fibrosis and success of catheter ablation by speckle tracking echocardiography in patients imaged in persistent atrial fibrillation. *Front Cardiovasc Med*. 2022;9:856796.

14. Voigt N, Li N, Wang Q, et al. Enhanced sarcoplasmic reticulum Ca2+ leak and increased Na+-Ca2+ exchanger function underlie delayed afterdepolarizations in patients with chronic atrial fibrillation. *Circulation*. 2012;125:2059-2070.

15. van Bragt KA, Nasrallah HM, Kuiper M, Luiken JJ, Schotten U, Verheule S. Atrial supply-demand balance in healthy adult pigs: coronary blood flow, oxygen extraction, and lactate production during acute atrial fibrillation. *Cardiovasc Res*. 2014;101:9-19.

16. Mason FE, Pronto JRD, Alhussini K, Maack C, Voigt N. Cellular and mitochondrial mechanisms of atrial fibrillation. *Basic Res Cardiol*. 2020;115:72.

17. Ausma J, Wijffels M, Thone F, Wouters L, Allessie M, Borgers M. Structural changes of atrial myocardium due to sustained atrial fibrillation in the goat. *Circulation*. 1997;96:3157-3163.

18. Gerber BL, Vanoverschelde JL, Bol A, et al. Myocardial blood flow, glucose uptake, and recruitment of inotropic reserve in chronic left ventricular ischemic dysfunction. Implications for the pathophysiology of chronic myocardial hibernation. *Circulation*. 1996;94:651-659.

19. Barth AS, Merk S, Arnoldi E, et al. Reprogramming of the human atrial transcriptome in permanent atrial fibrillation: expression of a ventricular-like genomic signature. *Circ Res*. 2005;96:1022-1029.

20. Gaborit N, Steenman M, Lamirault G, et al. Human atrial ion channel and transporter subunit gene-expression remodeling associated with valvular heart disease and atrial fibrillation. *Circulation*. 2005;112:471-481.

21. Goette A, Lendeckel U. Atrial cardiomyopathy: pathophysiology and clinical consequences. *Cells*. 2021;10:2605.

KEY WORDS atrial fibrillation, atrial cardiomyopathy, FDG-PET, glucose metabolism